Intergrowth $Bi_2WO_6-Bi_3TiNbO_9$ ferroelectrics with high ionic conductivity

Z. G. Yi[a] and Y. X. Li[b]
State Key Laboratory of High Performance Ceramics and Superfine Structures, Shanghai Institute of Ceramics, Chinese Academy of Sciences, 1295 Dingxi Road, Shanghai 200050, People's Republic of China

Z. Y. Wen and S. R. Wang
Advanced Functional Ceramic Engineering Research Center, Shanghai Institute of Ceramics, Chinese Academy of Sciences, 1295 Dingxi Road, Shanghai 200050, People's Republic of China

J. T. Zeng[a] and Q. R. Yin
State Key Laboratory of High Performance Ceramics and Superfine Structures, Shanghai Institute of Ceramics, Chinese Academy of Sciences, 1295 Dingxi Road, Shanghai 200050, People's Republic of China

(Received 10 December 2004; accepted 13 April 2005; published online 3 May 2005)

Two dielectric relaxation loss peaks associated with oxygen-ion diffusion in the intergrowth $Bi_2WO_6-Bi_3TiNbO_9(Bi_5TiNbWO_{15})$ bismuth layered ferroelectrics were observed. The activation energy and the relaxation time at infinite temperature, for these two peaks, were determined to be (0.89 eV, 1.3×10^{-13} s) and (0.84 eV, 3.6×10^{-10} s). The ac impedance spectroscopy indicated that the $Bi_5TiNbWO_{15}$ ceramic is an ionic conductor with an electrical conductivity of approximately 2.6×10^{-2} S/cm at a temperature of 1073 K. © *2005 American Institute of Physics*.
[DOI: 10.1063/1.1925760]

The family of mixed bismuth layer-structured oxides (BLSOs), has been the focus of much interest in regard to the relationship between their crystal structure and their ferro- or piezoelectric properties.[1–4] These types of compounds are usually made up of an intergrowth of one-half of the unit cell of a usual BLSO, and one-half of the unit cell of another BLSO along each *c* axis, with the difference of the numbers of perovskitelike layers that sandwiched between $(Bi_2O_2)^{2+}$ layers equals unity $(m-n=1)$. For example, the mixed BLSOs $Bi_5TiNbWO_{15}$, $Bi_7Ti_4NbO_{21}$, and $PbBi_8Ti_7O_{27}$ are made up of Bi_3TiNbO_9 $(m=2)$ and Bi_2WO_6 $(n=1)$, $Bi_4Ti_3O_{12}$ $(m=3)$ and Bi_3TiNbO_9 $(n=2)$, and $PbBi_4Ti_4O_{15}$ $(m=4)$ and $Bi_4Ti_3O_{12}$ $(n=3)$ along each *c* axis, respectively.

Since the discovery of these naturally heterostructures, it has been found that the piezoelectric property of $Bi_7Ti_4NbO_{21}$ and the ferroelectric property of $ABi_8Ti_7O_{27}$ (A=Pb, Sr) are enhanced when compared to their composed BLSOs.[3–5] However, the structure and electrical properties of $Bi_2WO_6-Bi_3TiNbO_9$ (BW–BTN) system require much further exploration.[1,6]

Low dielectric loss is a necessary requirement for the application of ferroelectric materials. However, the dielectric dissipation of BW–BTN ceramic is prominent especially at high temperature.[1,7] In view of the fact that electrical properties are of fundamental importance for ferroelectric devices applications, in this letter, dielectric relaxation and ac impedance spectroscopy are used to probe the nature of the high dielectric dissipation of BW–BTN ferroelectric ceramics.

The wafer specimens of BW–BTN with a diameter of 13 mm and a thickness of 1 mm were prepared by conventional solid-state reaction method. Appropriate amounts of high-purity raw materials were first mixed and presintered at 850 °C for 7 h, then pressed into pellets and sintered at 1040 °C in air for 4 h. The X-ray diffraction (XRD) patterns of sintered specimens were recorded using Cu $K\alpha$ radiation in a Rigaku D/max-2550V [scanning from 5° to 80° (2θ), using a step of 0.02° and counting time of 3 s for each step]. For electrical measurements, the pellets surfaces were polished prior to applying platinum electrodes. The alternating current electrical properties of the specimens were measured by an HP4194A and a Solartron 1260 impedance analyzer in air at a heating rate of 3 °C/min.

Figure 1 shows the Rietveld refined results for the BW–BTN powders. The XRD pattern was calculated under the assumption that BW–BTN has an intergrowth structure as depicted above with a space group of $Pmc2_1$. The *R*-weighted pattern (R_{wp}) was 16.2% and the goodness of fit (S) was 1.5. It can be seen that all diffraction peaks can be well indexed by the space group $Pmc2_1$ though the *R*-weighted pattern is a little large. The refined lattice constants *a*, *b*, and *c* are 2.0886(8) nm, 0.5429(5) nm, and 0.5406(4) nm, respectively. These lattice constants are the average of those of the constituent compounds of BW and BTN, respectively. More detailed structure information will be investigated further by neutron diffraction.

Figure 2 shows the variation of dielectric loss with frequency at different temperatures. Two dielectric loss peaks can be seen in Fig. 2(a). Though, the higher-frequency peak (denoted as P_{d1}) is not as obvious from this graph as the lower-frequency one (denoted as P_{d2}), the P_{d1} peak does exist and this is demonstrated clearly in Fig. 2(b). Owing to the elimination of the influence of P_{d2} peak, P_{d1} peak becomes distinct in a lower-temperature range. With increasing temperature, the positions of both peaks shift to a higher frequency. Corresponding to P_{d1} and P_{d2}, this is evident in Fig. 3, where two prominent dielectric loss peaks are also observed in dielectric loss versus temperature. These phenomena indicate that the two loss peaks are of relaxation characteristic and associated with a thermally activated relaxation process.

[a]Graduate School of the Chinese Academy of Sciences, Beijing 100039, People's Republic of China.
[b]Electronic mail: yxli@mail.sic.ac.cn

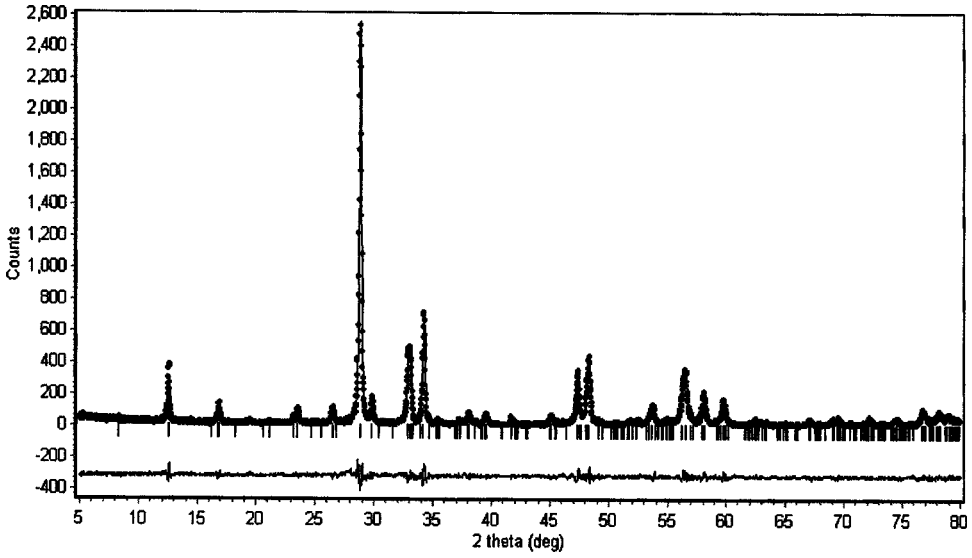

FIG. 1. XRD patterns and the Rietveld refinement for $Bi_5TiNbWO_{15}$ powders, where the solid circles are data points, the thin solid line is the refinement result, the short bars are the position of the diffraction peaks predicted from the space group $Pmc2_1$, and the thick line below is the difference between the data points and the fitted line.

For a thermally activated relaxation process, the activation energy (E) is generally related to the relaxation time τ through the Arrhenius law:

$$\tau = \tau_0 \exp(E/k_B T), \tag{1}$$

where τ_0 is the pre-exponential factor (or the relaxation time at infinite temperature), T is the absolute temperature, and k_B is Boltzmann constant. It is well known that at the peak position the condition $\omega_p \tau_p = 1$ is fulfilled, where $\omega = 2\pi f$ is the angular frequency of measurement, and the subscript p denotes values at peak position. Therefore, if we plot $\ln(\omega_p)$ as a function of the reciprocal of peak temperature (Arrhenius plots), a linear relation would be obtained and the relaxation parameters E and τ_0 can thus be deduced. The so-called Arrhenius plots for the two dielectric loss peaks are shown in Fig. 3, where the solid lines present the linear least-square fittings. From this figure, the relaxation parameters $E_1 = 0.89$ eV, $\tau_{01} = 1.3 \times 10^{-13}$ s for the P_{d1} peak, and $E_2 = 0.84$ eV, $\tau_{02} = 3.59 \times 10^{-10}$ s for the P_{d2} peak are obtained from these fitting lines. The values of the relaxation parameters are in the same range as those for oxygen ion diffusion in oxide ceramics[8,9] suggesting a mechanism of short distance diffusion of oxygen ions via vacancies for the P_{d1} and P_{d2} peaks.

Figure 4(a) presents the impedance spectra of the BW–BTN specimen measured at different temperatures in air. When the temperature equals 574 K, from high frequency to low frequency, there are three semicircles attributed to bulk, grain boundary, and electrode resistance, respectively. With the increasing of temperature, these three semicircles shift to higher frequency.

The electrical conductivity of the specimen can be calculated from the interceptions of the observed semicircles on

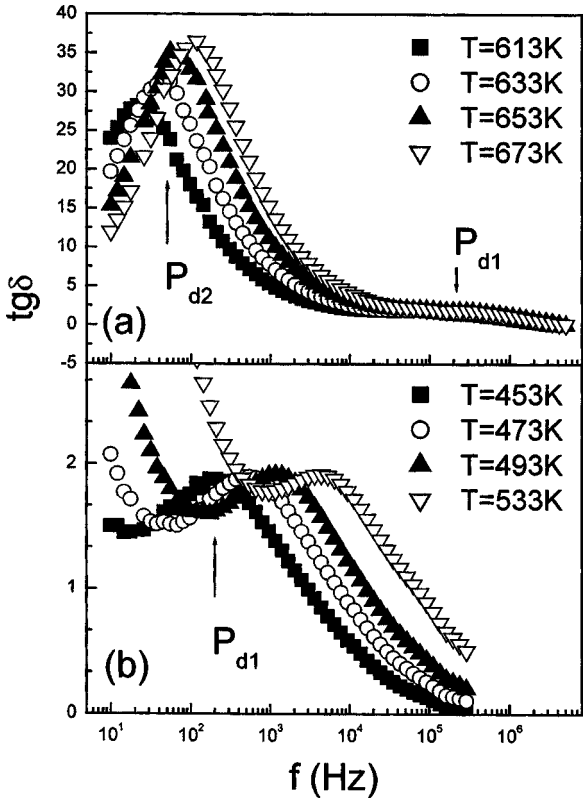

FIG. 2. (a) Frequency dependence of the dielectric loss for the $Bi_5TiNbWO_{15}$ specimen measured at different temperatures. (b) Frequency dependence of P_{d1} peak at a lower temperature range.

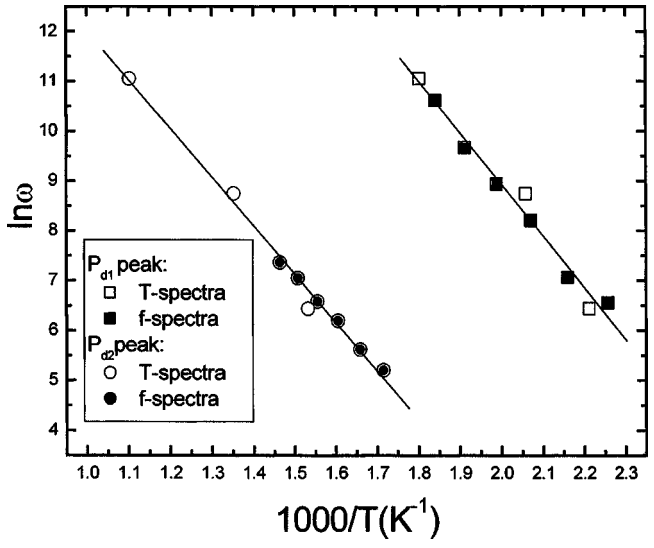

FIG. 3. The Arrhenius plot of the two dielectric loss peaks (P_{d1} and P_{d2}) from the frequency spectra (solid symbols) and temperature spectra (open symbols). The ordinate $\ln \omega$ is the exponential logarithm of measuring angular frequency. The solid lines are linear least-square fittings.

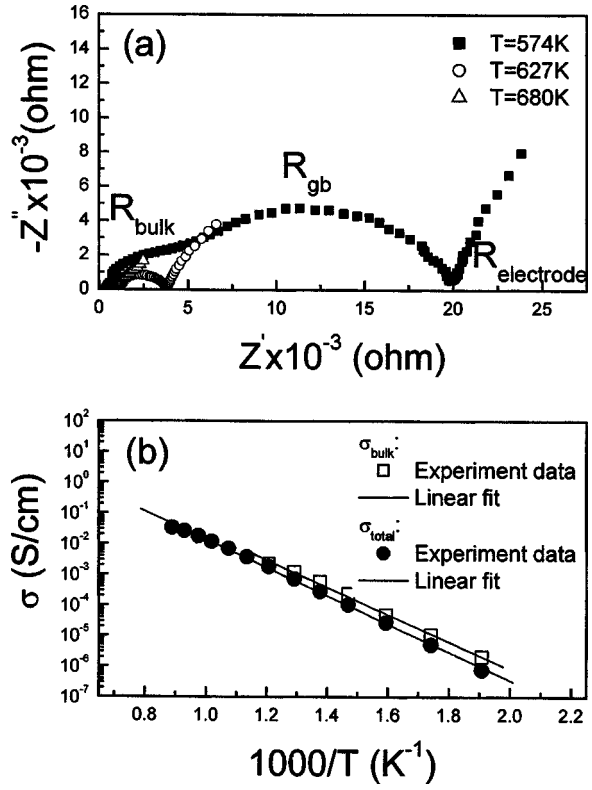

FIG. 4. (a) ac impedance spectra of the $Bi_5TiNbWO_{15}$ specimen measured at three different temperatures. (b) The bulk and total conductivity for the $Bi_5TiNbWO_{15}$ ceramic as a function of inverse temperatures. Solid lines show the Arrhenius temperature dependence.

the real axis of the impedance spectra. Figure 4(b) shows the Arrhenius plots of $\log \sigma$ versus $1000/T$ for the specimen. From the fitting lines, it can be seen that the conductivity data obey the Arrhenius law quite well in the temperature range from 523 K to 1123 K. The total conductivity at 1073 K is about 2.6×10^{-2} S/cm, and the grain conductivity at 823 K can reach 2×10^{-3} S/cm. The activation energies are 0.91 eV and 0.88 eV, respectively, which are in accordance with the activation energies calculated from above dielectric loss spectroscopy. The reason that the activation energy calculated from total conductivity versus the reciprocal of temperature is slightly larger than that of grain conductivity is that the former includes the contribution of grain boundaries. It is well known and widely accepted that vacancy hopping is the common mechanism in solid-state ionics. Hence, the high electrical conductivity at high temperature, which is comparable to $Bi_2Sr_2Nb_2GaO_{11.5}$, a little larger than $Bi_2Sr_2Nb_2AlO_{11.5}$, $Bi_2Sr_2Ta_2GaO_{11.5}$,[10] and Bi_2WO_6,[11] demonstrates that the material BW–BTN is also a superionic conductor.

In order to establish if the material was an oxide ion conductor, the impedance spectra experiment was employed under different gas atmospheres at 650 °C. Changing the gas atmosphere from oxygen to air and to nitrogen, the conductivity of BW–BTN decreased only slightly. However, in a hydrogen atmosphere, the conductivity increased quickly and the sample was chemically reduced and became black. Though the behavior observed at higher oxygen concentrations (from oxygen to air and to nitrogen) was similar to $Bi_4Ti_3O_{12}$,[12] revealing that BW–BTN was an ionic *p*-type mixed conductor, the electron or hole contribution to the total conductivity is minimal. This result, associated with the dielectric spectroscopy experiments mentioned above, confirmed the suggestion that the two prominent dielectric loss peaks originate from oxygen vacancy relaxation.

In the BLSOs, it is generally believed that $(Bi_2O_2)^{2+}$ layers act as insulating layers and oxygen diffusion at a high temperature is through the pseudo-perovskite layers. However, there was lack of convincing experimental evidence along $a(b)$-axis for a long time. Recently, Yasuda *et al.*[13] investigated the layer-structured $Bi_4V_{2(1-x)}Co_{2x}O_{11-\delta}$ ($x=0.0-0.1$) single crystals by impedance analysis and revealed that the electrical anisotropy do indeed result from the highly conductive perovskite block. But, for the intergrowth BW–BTN ferroelectrics, do they also include highly conductive perovskite layers? In view of the oxygen ion conductors $Bi_2VO_{5.5}$, $Bi_4V_2O_{11}$,[14] $Bi_2Sr_2Nb_2GaO_{11.5}$, and $Bi_2Sr_2Ta_2GaO_{11.5}$,[10] there are intrinsic oxygen vacancies or extrinsic oxygen vacancies that are introduced by doping into the perovskite. For BW–BTN ceramics, are there intrinsic oxygen vacancies? Maybe the following simple consideration is helpful to understand its high oxygen ion conductivity: It seldom avoids the volatilization of bismuth during the fabrication of BLSOs at high temperature. To maintain electrical neutrality, oxygen vacancies will be generated both in the perovskite layers and $(Bi_2O_2)^{2+}$ layers. However, to understand the mechanism of the oxygen ion or vacancy diffusion in detail, further theoretical analysis based on the crystal structure is necessary.

In summary, two dielectric loss peaks were observed in the BW–BTN ceramics, which are associated with oxygen ion diffusion. The impedance spectra experiments indicated that the intergrowth ferroelectric BW–BTN is a superionic conductor and has potential applications in solid oxide fuel cells, oxygen sensors, oxygen pumps, oxygen-permeable membranes, catalysts, etc.

This work was supported by the Ministry of Science and Technology of China through 973-Project under Grant No. 2002CB613307.

[1]T. Kikuchi, J. Less-Common Met. **48**, 319 (1976).
[2]Y. Noguchi, M. Miyayama, and T. Kudo, Appl. Phys. Lett. **77**, 3639 (2000).
[3]Y. Goshima, Y. Noguchi, and M. Miyayama, Appl. Phys. Lett. **81**, 2226 (2002).
[4]J. Zhu, X. B. Chen, W. P. Lu, X. Y. Mao, and R. Hui, Appl. Phys. Lett. **83**, 1818 (2003).
[5]P. Durán, F. Capel, C. Moure, M. Villegas, J. F. Fernández, J. Tartaj, and A. C. Caballero, J. Eur. Ceram. Soc. **21**, 1 (2001).
[6]Y. Noguchi, R. Satoh, M. Miyayama, and T. Kudo, Jpn. J. Ceram. Soc. **109** 29 (2001).
[7]A. Lisińsha-Czekaj, D. Czekaj, Z. Surowiak, J. Ilczuk, J. Plewa, A. V. Leyderman, E. S. Gagarina, A. T. Shuvaev, and E. G. Fesenko, J. Eur. Ceram. Soc. **24**, 947 (2004).
[8]M. Weller and H. Schubert, J. Am. Ceram. Soc. **69**, 573 (1986).
[9]C. Ang, Z. Yu, and L. E. Cross, Phys. Rev. B **62**, 228 (2000).
[10]K. R. Kendall, J. K. Thomas, and H. C. zur Loye, Chem. Mater. **7**, 50 (1995).
[11]T. Takahashi and H. Iwahara, J. Appl. Electrochem. **3**, 65 (1973).
[12]M. Takahashi, Y. Noguchi, and M. Miyayama, Solid State Ionics, **172**, 325 (2004).
[13]N. Tasuda, M. Miyayama, and T. Kudo, Mater. Res. Bull. **36**, 323 (2001).
[14]J. C. Boivin and G. Mairesse, Chem. Mater. **10**, 2870 (1998).